Channel Influence Mitigation in Pseudo-Noise Waveform Design for Radar Applications

Janusz S. KULPA

Institute of Electronic Systems, Warsaw University of Technology, Nowowiejska 15/19, 00-665 Warsaw, Poland

J.Kulpa@elka.pw.edu.pl

Abstract. *Noise Radar is a rapidly developing technology which uses noise or pseudo-noise waveforms as sounding signals to detect targets of interest. The advantages of such waveforms are no range nor velocity ambiguities, the possibility of using continuous waveform and low probability of intercept. However, the noise waveform correlation sidelobes are spread across the entire range–Doppler plane and their level is determined by the time-bandwidth product. Such sidelobes limit the detection capability in the multitarget environment. Several algorithms exist that decrease the sidelobe level and thus enhance dynamic range of the radar, but they are very susceptible to distortions in an analogue channel. In this paper the author presents a method to create low-sidelobe waveforms using a filtering algorithm designed for given channel, decreasing the analogue front-end impact on the final properties of the waveforms.*

Keywords

Noise radars, random signal radar, zero correlation zone, waveform design, channel calibration.

1. Introduction

Continuous Wave (CW) Radars have become very popular nowadays. The main reason is the power budget. To obtain a similar detection range, the total emitted energy must be the same both in pulse and CW radars. As a result, the CW radar has a much lower peak to average power ratio than its pulse counterpart, usually close to one. Thus, CW radars' transmitter are simpler. In many systems, mainly because of system complexity and price, the Frequency Modulated Continuous Wave (FMCW) [1] is used. The compressible waveform offers the possibility of obtaining better dynamic range and detection accuracy. Among possible CW signals, noise-like waveforms offer very interesting properties.

The usage of noise signals prevents or limits both range and velocity ambiguities, and offers a low probability of intercept and classification of the radar (LPI properties) as well as good electromagnetic compatibility. Different noise-like signals may be used as sounding waveforms, both natural noise, such as amplified thermal noise, or deterministic pseudo-noise generated digitally. Various amplitudes' distributions may be applied including Gaussian, limited Gaussian, uniform or unimodular amplitude distributions, where usually phase distribution is uniform.

The Noise Radar idea was introduced in the late '50s [2], and some prototypes were built. Different ideas of signal processing were proposed ranging from spectrum, anti-correlation and correlation analyses [3]. The development of such systems was limited due to system accuracy and technical capabilities. Only recently, mainly due to an increase in computational power and the improvements in analogue front-ends, the Noise Radar is becoming a topic of interest for many research institutes [4, 5, 6].

Modern noise radar solutions are based on correlation analyses. Although the analogue noise radar may be built [7], digital signal processing offers much better performance and flexibility, including clutter cancellation techniques [8] and CLEAN algorithm applicability [9]. Noise Radar is very susceptible to the masking effect due to the nature of the point spread function (PSF) of a noise waveform, which is the autoambiguity function of a transmitted signal [10]. The sidelobes of PSF are spread across the entire range-Doppler plane at the level of the time-bandwidth product below the main lobe. Let us consider an example. For integration time T_{int} = 7 ms and bandwidth B = 36 MHz the sidelobe level is around -54 dB. This value is often not sufficient for weak target detection and calculation of CLEAN algorithms is computationally expensive.

The other method for dynamic range improvement, where the computational burden is moved to the system design level or signal generating unit rather than post–recording signal processing, is the usage of waveforms with lower correlation sidelobes. The well known codes with low correlation are, among others, Barker [11], Frank [12] and Costas codes [13] for pulse waveforms and M-sequences for continuous waveforms. However, for a given code type and signal length, only a few different realizations exist at best and such solutions do not possess good LPI or electromagnetic compatibility properties. This is especially troublesome if several transmitters are placed in proximity, leading to severe interferences and false detections. Among various other signals, the Multi-sine with randomized phase [14] is

a waveform type with good correlation and LPI properties, however high peak to average power ratio of this signal may limit its usability.

In recent years much effort has been put into techniques that generate noise-like waveforms with better correlation properties. Some of them use transformation of sequences with good correlation properties [15], others start with pseudo-random sequences and optimize them to obtain the desired ambiguity function [16, 17, 18] or perform filtering with a dedicated filter [19]. All of them try to obtain a good autoambiguity function using either a constraint on function value for non-zero delay or integrated sidelobes level criteria.

The autocorrelation function of the mentioned waveforms might be degraded due to distortion in a real channel. The main goal then should be to design signals which have good properties after propagating through the channel, not before the propagation. In this field, apart from [20], not much research has been carried out yet.

In this paper an improvement for filtering-based waveform design [21] is shown which mitigates the distortions introduced by the analogue channel without its explicit estimation. The simulation analysis along with measurement data are shown.

The paper is organized as follows: Section 2 describes the properties of the noise ambiguity function and outlines the algorithm of the filtering-based waveform design presented in [21]. Section 3 shows the influence of a non-perfect channel. In Section 4 the algorithm for channel influence mitigation is introduced, along with simulations and measurement results. Section 5 concludes the paper.

2. Ambiguity Function

Noise Radar, as most other CW radars, requires separate transmit and receive antennas. Noise waveform illuminates the observed scene and is scattered back to the radar. The received signal is then compared with the transmitted one, either in an analogue manner or digitally. Then, after preprocessing, the crossambiguity function is calculated:

$$\chi_{y_{tran}y_{rec}}(\tau, f_d) = \int_{t_s}^{t_s+T_{int}} y_{rec}(t) y^*_{tran}(t-\tau) e^{j2\pi f_d t} dt \quad (1)$$

where τ is time delay, f_d is the Doppler shift of the received signal t_s is a starting instant of integration and * is the complex conjugate operator. Digital processing is usually done blockwise, i.e. one block of length N, which corresponds to integration time T_{int}, is recorded.

The crossambiguity function of the received signal (1) is the superposition of the autoambiguity function of the transmitted signal y_{tran} ($\chi_{y_{tran}y_{tran}}(\tau, f_d)$) shifted in frequency and time corresponding to scattering points ranges and velocities with adequate amplitude scaling factor. The shape of the autoambiguity function of a noise-like signal is a thumbtack with sidelobes at the level of the time-bandwidth product ($B \cdot T_{int}$) of the transmitted waveform. Since the transmitted waveform is continuous, the echoes from all targets, both close and distant, are received simultaneously. The echoes of targets with small radar cross sections (RCS) or that are far from the radar may be completely masked by the sidelobes of strong echoes.

One method to overcome this problem is to use the waveform with reduced sidelobes. It is not necessary to suppress the crossambiguity function sidelobes on the entire range plane. Radars are designed for specified observation areas. The detection range is limited by transmitted power, receiver noise figure and antennas, and only the observation region needs suppressed sidelobes.

2.1 Sidelobes Reduction Technique

In [21] and [19] algorithm for range sidelobes reduction and its extension for range-Doppler plane were proposed by the author and his co-workers. In this paper the analysis will only consider the range sidelobes reduction algorithm.

With range-only processing, the ambiguity function may be replaced with a one dimensional correlation function given by

$$\mathrm{R}_{y_{tran}y_{rec}}(\tau) = \int_{t_s}^{t_s+T_{int}} y_{rec}(t) y^*_{tran}(t-\tau) dt. \quad (2)$$

The algorithm [21] focuses on altering the given noise signal to reduce its sidelobes for selected range bins and may be viewed as a cascade of finite impulse response (FIR) filters designed for certain noise realization. The order of i-th filter

$$H_i(z) = 1 + \sum_{m=0}^{M-1} b_{m_0+m}(i) z^{-m_0-m} \quad (3)$$

is $M + m_0 - 1$, which corresponds to maximum detection range, where M is the number of range bins with sidelobes suppressed, m_0 is guard zone as shown in Fig. 1 and $b_k(i)$ are i-th cascade FIR filter coefficients. For a radar with a bandwidth B = 36 MHz operating up to a range of 650 m the filter order should be no less than 78. The guard zone m_0 should be set beyond the main lobe to prevent major band and distribution alteration in the output signal.

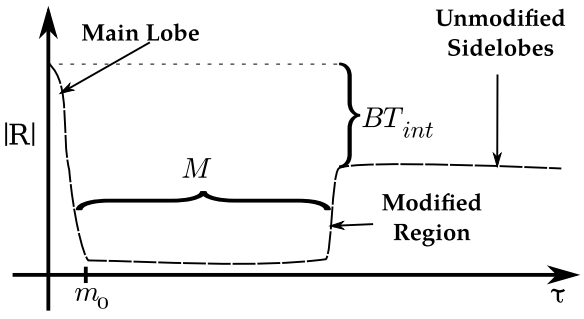

Fig. 1. The desired autocorrelation function.

Filter coefficients may be obtained from the assumption that the output signal correlation function is equal to 0 for desired time lags. It requires a solution of the polynomial

equation set, but the simplified solution for filter coefficients $b(i)$, neglecting higher order terms, is given by the equation

$$\begin{bmatrix} \mathrm{R}_i(m_0) \\ \mathrm{R}_i(m_0+1) \\ \vdots \\ \mathrm{R}_i(m_0+M-1) \end{bmatrix} = \mathbf{W}(i) \cdot \begin{bmatrix} b_{m_0}(i) \\ b_{m_0+1}(i) \\ \vdots \\ b_{m_0+M-1}(i) \end{bmatrix} \tag{4}$$

where R_i is the autocorrelation function of the i-th cascade input signal,

$$\mathbf{W}(i) = \begin{bmatrix} \mathrm{R}_i(0) & \mathrm{R}_i(-1) & \cdots & \mathrm{R}_i(-M+1) \\ \mathrm{R}_i(1) & \mathrm{R}_i(0) & \cdots & \mathrm{R}_i(-M+2) \\ \vdots & \vdots & \ddots & \vdots \\ \mathrm{R}_i(M-1) & \mathrm{R}_i(M-2) & \cdots & \mathrm{R}_i(0) \end{bmatrix}, \tag{5}$$

and if $m_0 > 1$,

$$b_1(i) = b_2(i) = \ldots = b_{m_0-1}(i) = 0. \tag{6}$$

The efficiency of a single filter with a simplified solution is usually tens dB in terms of sidelobes reduction level, but this value depends on singal length and the size of suppression area M. Additional cascades may be used for improvement of sidelobe reduction. The influence of the number of filters in the cascade on signal sidelobes suppression is presented in Fig. 2. One of advantages is that this algorithm may suppress the sidelobes of signals with various amplitude distributions, altering it only slightly.

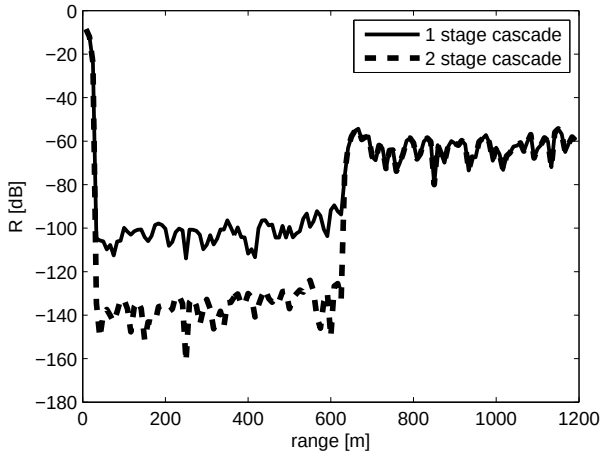

Fig. 2. Waveform design efficiency depending on number of filters in cascade.

A computationally efficient method to calculate both the ambiguity and correlation functions is via fast Fourier transform (FFT). This method assumes the cyclic nature of the waveform. The correlation of a non-full or non-cyclic block results in a slight increase of sidelobes in the modified area. To ensure maximum sidelobes reduction the cyclic prefix must be added, similar to one in Orthogonal Frequency–Division Multiplexing (OFDM) transmission. One needs to keep in mind that the tradeoff of better sidelobe suppresion is the lower probability of intercept.

3. Channel Influence

In a real environment the point spread function differs from the autoambiguity function of the transmitted waveform due to channel amplitude and phase distortions. Even if the signal is transmitted only in the passband of both receiver and transmitter, minor ripples in channel frequency response may exist and alter the ambiguity function in the area of interest. Apart from this, if the transmitted waveform has a flat power density function in the digital domain, the autoambiguity is convolved with *sinc* function significantly increasing sidelobes, especially for close ranges. This effect is usually not strictly visible in the digital domain since zeros of *sinc* function correspond exactly to correlation range bins but this effect needs to be considered in a operational system. To reduce the time sidelobes dependent on signal spectrum, all signals presented in this paper have the Hann window applied in the frequency domain.

To analyze the channel influence on the correlation function, simulations were performed. The center frequency was set to 1.95 GHz. The complex Gaussian pseudo-noise x_g of length $N \approx 320000$ samples with 36 MHz bandwidth and 46.08 MHz sampling frequency was generated. The signal was filtered by a cascade of filters designed for its sidelobe suppression (3) with total transfer function $H_s(z)$ and a signal with suppressed sidelobes x_s was obtained. Then this modified noise was transferred through the pass-band of the channel filter $H_{ch}(z)$ resulting in the x_{sch} signal. The signal flow idea along with an approximated autocorrelation function is shown in Fig. 3.

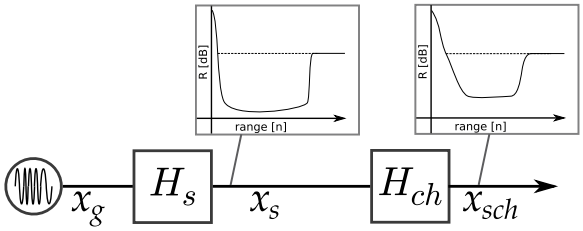

Fig. 3. Idea of signal flow through channel.

In the simulation two exemplary channel models were used: a type-I Chebyshev filter and an elliptic filter. Both filters were of 6-th order with 1 dB ripples in the pass band. The correlation function was calculated via FFT for all three signals, x_s (which may be viewed as a signal transferred through an ideal channel $H_{ch}(z) \equiv 1$), $x_{sch_{cheby}}$ and $x_{sch_{ellip}}$ (transferred through a non-ideal channel). As a reference signal in the correlation function, a copy of the corresponding signal time-shifted by 2.5 samples was used. The half–sample time shift is the worst case scenario for a filtering based algorithm since it focuses sidelobes suppression on integer delays. The correlation functions are presented in Fig. 4. One can see that even ripples in the pass band as small as 1 dB may not only significantly increase the entire sidelobes region, but also widen the main lobe.

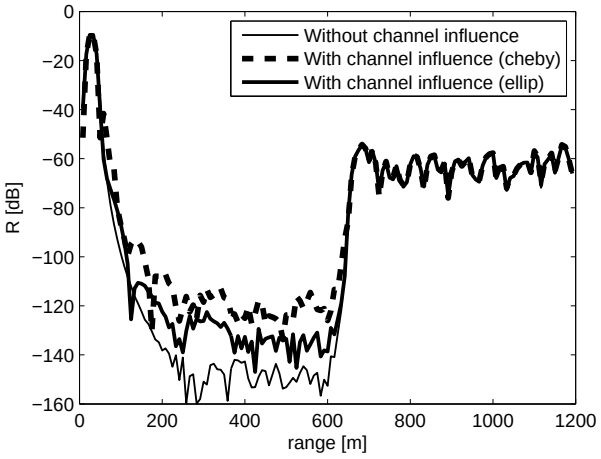

Fig. 4. Channel influence on correlation function.

4. Channel Influence Mitigation

The classical approach to the channel influence problem is to design the inverse channel filter and apply it to the recorded signal. This approach may be difficult since it is necessary to estimate the channel transfer function $H_{ch}(z)$ and then design the inverse channel filter $H_{ch}^{-1}(z)$. This idea is presented in Fig. 5. If the transfer function of the channel model have zeros in z plane beyond unit circle, the inverse filter will be unstable due to its poles location. Even if the zeros are close to unit circle, but still inside it, the inverse filter is susceptible to numerical errors. The problem of numerical errors limits usage of methods like deconvolution.

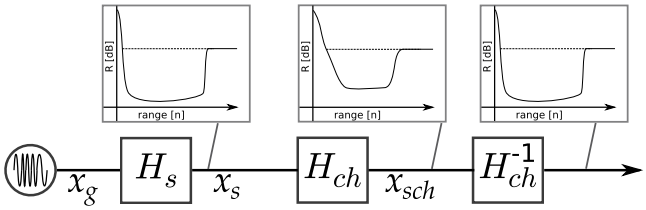

Fig. 5. Mitigation idea – classical approach.

The idea of channel influence mitigation presented in this paper does not require channel transfer function estimation. The only a priori assumption is that the channel is a linear time-invariant (LTI) system. The proposed algorithm consists of two stages: designing a sidelobe suppression filter (3) for a channel–distorted signal and preparing the initial sounding signal with a previously designed filter.

If the LTI assumption is valid, it is possible to reverse the filter order and design filter cascade $H_m(z)$ that suppresses the sidelobes of signal x_{ch}, which is obtained by propagating the initial signal x_g trough the channel ($H_{ch}(z)$). The signal x_{chm} is obtained by filtering the x_{ch} signal with $H_m(z)$ filter. The signal x_{chm} is expected to have narrow main lobe and suppressed sidelobes in desired area. The idea of filter design with expected correlation function is shown in Fig. 6.

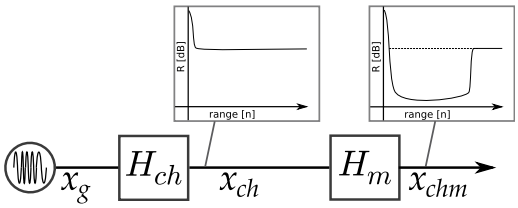

Fig. 6. Mitigation idea – filter design.

Since for an LTI system the following equation is valid,

$$H_m(z)\,(H_{ch}(z)\cdot\mathcal{Z}[x_g]) \equiv H_{ch}(z)\,(H_m(z)\cdot\mathcal{Z}[x_g]) \qquad (7)$$

where $\mathcal{Z}[x_g]$ is the Z-transform of signal x_g, applying the designed filter $H_m(z)$ to the initial signal x_g will result in signal x_m, which is designed for certain propagation channel $H_{ch}(z)$. This signal may be then used in radar surveillance mode and it is expected that after it propagates through the channel, its correlation function will be similar to the desired correlation function of the x_{chm} signal (Fig. 7).

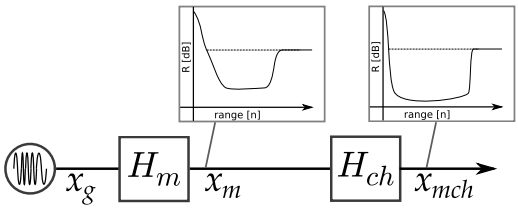

Fig. 7. Mitigation idea – filtering and surveillance.

4.1 Simulations

To verify the proposed method a set of simulations were performed. Most simulation parameters correspond to the ones described in chapter 3, with exception that only the type-I Chebyshev filter was used. The complex Gaussian pseudo-noise x_g signal was filtered by the channel filter $H_{ch}(z)$, resulting in the x_{ch} signal. Then the filtering-based algorithm was used to design a filter cascade with total transfer function $H_m(z)$ which suppresses the sidelobes of the x_{ch} signal. Filter coefficients were stored and the same filter was applied to the initial signal x_g and as a result the x_m signal was obtained. After transferring the modified signal (x_m) through the channel, the signal x_{mch} was obtained.

Similar to the previous situation, the correlation function of the x_{mch} signal with a copy of the x_{mch} signal time-shifted by 2.5 samples was calculated. In Fig. 8 the correlation function of the x_{mch} was compared against the correlation of the signal without channel correction x_{sch}. As it is shown, the mitigation algorithm shrinks the main lobe width to the level of the Hann window sidelobes.

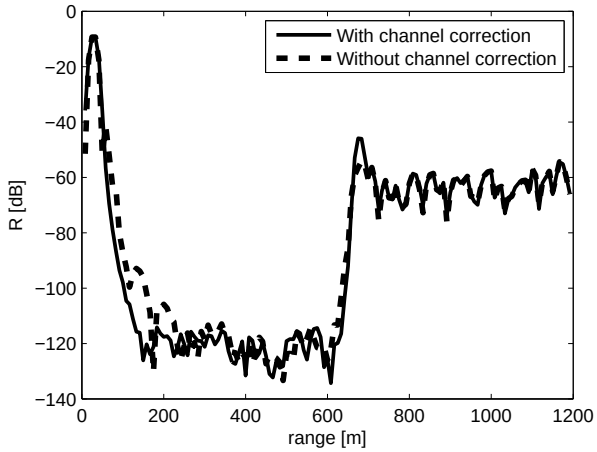

Fig. 8. Crosscorrelation function comparison (Simulations).

4.2 Measurements

To fully verify the proposed method, measurements were conducted. As a signal source the arbitrary waveform generator (AWG) Agilent MXG N5182A was used. The signal was split by a -20 dB directional coupler. The data were recorded on a 2-channel vector signal analyzer (VSA) Agilent VSA 89640 with a short cable used as a reference channel while a second, 15 meters long, was used as the surveillance. The generator and analyzer were synchronized by a common clock. The carrier frequency in the experiment was set to 1.95 GHz. The equipment pass band used in the experiment is equal to 36 MHz, although up to 1 dB of ripples existed in the frequency spectrum. The sampling frequency of both AWG and VSA was set to 46.08 MHz. The system setup is presented in Fig. 9.

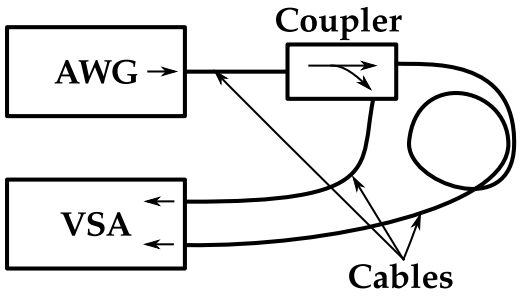

Fig. 9. Measurement setup.

The measurement scheme was similar to the simulations performed. First, the $N \approx 320000$ samples of complex Gaussian pseudo-noise were generated. For a future comparison, the waveform design of the initial signal was performed. As a result the x_s signal was obtained. This signal was uploaded to the AWG and recorded as the x_{sch}. Each uploaded signal was repeated continuously, but it is not necessary if a trigger signal is used along with the OFDM-like prefix described in Section 2. Afterward the initial x_g signal was also uploaded to the AWG and recorded as x_{ch}. The channel-dependent filter $H_m(z)$ was obtained on the basis of the x_{ch} signal. Then the initial noise signal x_g was filtered using the $H_m(z)$ filter to obtain the x_m signal. Finally, the latter signal was uploaded to the AWG and recorded as x_{mch}.

The crosscorrelation between the surveillance and reference channels was calculated for both the unmodified algorithm (signal x_{sch}) and channel dependent algorithm (signal x_{mch}). Both functions are presented in Fig. 10. It is clearly visible that without the channel mitigation technique the sidelobes close to the main lobe are about 30 dB higher. The main lobe of the correlation function was shrunk by 9 samples, which corresponds to resolution improvement by 75 m.

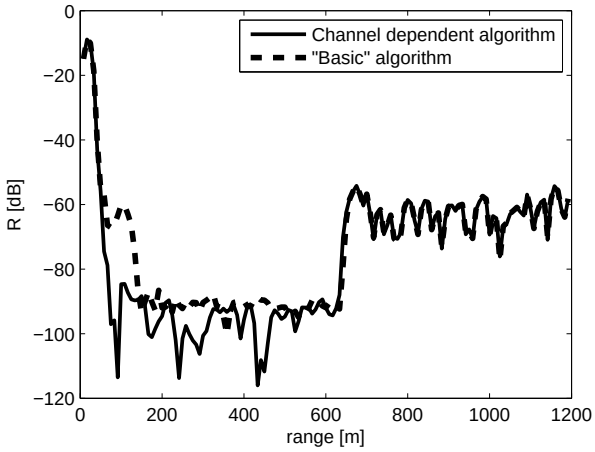

Fig. 10. Crosscorrelation function comparison (Measurements).

The difference in level of the suppressed sidelobes between the measurements and the simulation is caused by the numerical accuracy of the signal representation since the quantization noise is added. In this experiment the limitation is due to the effective number of bits of VSA used, which is approximately 12.

5. Conclusions

In this paper, channel influence on suppressed correlation sidelobes of a pseudo-noise waveform used in noise radar was shown along with a method to mitigate this influence.

Even small ripples in the pass-band of the radar analogue front-end may increase the sidelobes of the correlation function suppressed in the waveform design algorithm and widen the correlation main lobe, decreasing the overall efficiency of the sidelobe suppression method. By introducing an additional step in the filtering–based waveform design algorithm it is possible to shrink the main lobe to its initial width without the necessity to estimate channel transfer function, as shown in both simulations and measurements.

The aim of future work is to extend the presented algorithm for 2-dimensional range-Doppler ambiguity function improvement.

Acknowledgements

This work was partially supported by the Polish Ministry of Science and Higher Education through the science budget for 2012-2015 under the research program „Diamentowy Grant", project no. 0009/DIA/2012/41.

References

[1] BINNS, P. FMCW radar: a low cost sensor for automotive applications. In *IEE Colloquium on Automotive Sensors*. 1992, p. 6/1 - 6/6.

[2] HORTON, B. Noise-modulated distance measuring systems. *Proceedings of the IRE*, 1959, vol. 47, no. 5, p. 821 - 828.

[3] GUOSUI, L., HONG, G., XIAOHUA, Z., WEIMIN, S. The present and the future of random signal radars. *IEEE Aerospace and Electronic Systems Magazine*, 1997, vol. 12, no. 10, p. 35 - 40.

[4] LUKIN, K. Millimeter wave noise radar technology. In *Third International Kharkov Symposium on Physics and Engineering of Millimeter and Submillimeter Waves (MSMW)*. Kharkov (Ukraine), 1998, vol. 1, p. 94 - 97.

[5] THAYAPARAN, T., DAKOVIĆ, M., STANKOVIĆ, L. Mutual interference and low probability of interception capabilities of noise radar. *IET Radar, Sonar Navigation*, 2008, vol. 2, no. 4, p. 294 - 305.

[6] LIEVSAY, J., AKERS, G. Moving target detection via digital time domain correlation of random noise radar signals. In *IEEE Radar Conference (RADAR)*. 2011, p. 784 - 788.

[7] SUSEK, W., STEC, B., RECKO, C. Broadband microwave correlation receiver for noise radar. In 11^{th} *International Radar Symposium (IRS)*. 2010, p. 1 - 4.

[8] KULPA, K., CZEKAŁA, Z. Short distance clutter masking effects in noise radars. *Applied Radio Electronics*, 2005, vol. 4, no. 1, p. 96 - 98.

[9] KULPA, K. The CLEAN type algorithms for radar signal processing. In *Microwaves, Radar and Remote Sensing Symposium (MRRS)*. 2008, p. 152 - 157.

[10] WOODWARD, P. M.*Probability and Information Theory, with Applications to Radar.*. London: Pergamon Press ltd., 1953.

[11] BARKER, R. H. Group synchronization of binary digital systems. In *Proceedings of Second London Symposium on Information Theory*. 1953, p. 273 - 287.

[12] FRANK, R. L. Polyphase codes with good nonperiodic correlation properties. *IEEE Transactions on Information Theory*, 1963, vol. 9, no. 1, p. 43 - 45.

[13] COSTAS, J. A study of a class of detection waveforms having nearly ideal range-Doppler ambiguity properties. *Proceedings of the IEEE*, 1984, vol. 72, no. 8, p. 996 - 1009.

[14] SACHS, J. *Handbook of Ultra-Wideband Short-Range Sensing: Theory, Sensors, Applications*. Wiley, 2013.

[15] HAYASHI, T., MAEDA, T., KANEMOTO, S., OKAWA, S. Zero-correlation zone sequence sets having subsets and its application to instrumentation. In *Proceedings of SICE Annual Conference (SICE)*. 2011, p. 2406 - 2410.

[16] MATHELIER, B., KIRAN, D., REDDY, V. U. Synthesis of waveforms from zero-lag cross-correlation matrix with specified constraints and power levels. In *International Conference on Signal Processing and Communications (SPCOM)*. 2012, p. 1 - 4.

[17] HE, H., STOICA, P., LI, J. Unimodular sequence design for good autocorrelation properties. In *IEEE International Conference on Acoustics, Speech and Signal Processing (ICASSP)*. 2009, p. 2517 - 2520.

[18] STOICA, P., HE, H., LI, J. New algorithms for designing unimodular sequences with good correlation properties. *IEEE Transactions on Signal Processing*, 2009, vol. 57, no. 4, p. 1415 - 1425.

[19] KULPA, J. S., MISIUREWICZ, J. Pseudo-noise waveform design minimizing range and Doppler masking effect. *International Journal of Electronics and Telecommunications*, 2011, vol. 57, no. 3, p. 359 - 362.

[20] ANGLIN, J., STILES, J. Radar transmit waveform design for lossy propagation channels. In *International Waveform Diversity and Design Conference (WDD)*. 2010, p. 121 - 125.

[21] KULPA, J. S., MAŚLIKOWSKI, Ł., KULPA, K. Pseudo-noise waveform synthesis for SAR applications. In *European Radar Conference (EuRAD)*. 2010, p. 25 - 28.

About Author ...

Janusz S. KULPA was born in 1988 in Białystok, Poland. He received his B.Sc. and M.Sc. in Electrical and Computer Engenieering from the Warsaw University of Technology in 2011 and 2013 respectively. He is currently doing his Ph.D. and working as a research assistant at the Warsaw University of Technology. His research interests include passive radars, noise radars and compressive sampling.